

## WCRC-8 SPECIAL ISSUE ENGINEERING & GINNING

### Production of Furfural from Cottonseed Hulls: A Sustainable Approach for Cotton By-Product Utilization

Manoj Kumar\*, Jyoti Singh, Kanika Sharma, Charlene P. D'Souza, Ajinath Dukare,  
Leena Nehete, and Sujata Saxena

#### ABSTRACT

The use of lignocellulosic biomass to produce value-added chemicals like furfural, a platform chemical typically produced via acid-catalyzed dehydration of pentose sugars derived from hemicellulose, is gaining attention in the biorefinery industry. Cottonseed hulls (CSH), an abundant by-product of the cotton industry, represent a promising source for furfural production due to relatively higher hemicellulose content (11.6–24.5%) in comparison to hemicellulose content of other lignocellulosic biomasses such as wheat bran (22%), bagasse (16.52%), and hemp (10.60%). The objective of this study is to optimize the furfural production process using Box-Behnken design (BBD), a response surface methodology, to maximize furfural yield from CSH. The effects of three critical variables on furfural yield were systematically investigated: pre-treatment using varying ratios (5:1–15:1) of 1% H<sub>2</sub>SO<sub>4</sub> to CSH (1% H<sub>2</sub>SO<sub>4</sub>:CSH); acid hydrolysis using varying concentration (2.5–7.5%) of H<sub>2</sub>SO<sub>4</sub> to CSH (% H<sub>2</sub>SO<sub>4</sub>:CSH); and reaction time ranging from 30 to 90 min. Statistical analysis using ANOVA confirmed the model significance ( $p < 0.05$ ) and revealed that all three variables (either individual or interaction) had significant effects on furfural yield. The optimized process conditions: pretreatment of 11.731 (1% H<sub>2</sub>SO<sub>4</sub>:CSH), acid hydrolysis of 6.74% (% H<sub>2</sub>SO<sub>4</sub>:CSH), and a reaction time of 81.2 min with desirability 1 resulted in a furfural yield of 14.34%. The study successfully demonstrates the application of BBD in optimizing the production of furfural from CSH, thus enhancing

its potential as an economically viable feedstock for the biorefinery industry contributing to the advancement of biomass conversion technologies for the sustainable production of high-value chemicals.

Cotton is a major global agricultural commodity, with an annual cotton fiber production of more than 25 million tons (Voora et al., 2023). Moreover, as a crucial oil crop, it generates 41 million tons of cottonseed processed into oil and meal, and its hulls, amounting to millions of tons, are used as animal feed, renewable energy, and mushroom cultivation substrates (Desrochers and Szurmak, 2017; USDA ERS, 2014). Lignocellulosic biomass is viewed as a sustainable feedstock because of its renewability, abundance, and wide distribution. It is mainly composed of polysaccharides (30–50% cellulose, 20–35% hemicellulose, 15–30% lignin), which can be converted to useful products via several intermediate molecules (e.g., levulinic acid [LA], furfural [FF]) (Lu et al., 2023).

Hemicellulose is a complex and vital component of the plant cell wall, associated with cellulose, lignin, and other compounds. Hemicelluloses, being hydrophilic with a lower degree of polymerization and higher solubility compared to cellulose, are more susceptible to hydrolysis, which facilitates their use in producing biomass derivatives. Their structural diversity enables the production of various compounds through multiple conversion pathways (Ajao et al., 2018; Luo et al., 2019). Due to its recalcitrance, pretreatment strategies tailored to each raw material's composition and target products are necessary, often requiring a combination of biomass fractionation methods (Scapini et al., 2021). Xylans are the predominant hemicellulose in hardwood biomass, playing a key role in the composition and structure of the secondary cell wall, which is linked to biomass recalcitrance (Wierzbicki et al., 2019). Effective use of hemicellulose in lignocellulosic biomass involves

M. Kumar\*, J. Singh, K. Sharma, C.P. D'Souza, A. Dukare, L. Nehete, and S. Saxena, Chemical and Biochemical Processing Division, ICAR – Central Institute for Research on Cotton Technology, Mumbai, 400019, India

\*Corresponding author: manojkumarpunia114@gmail.com

selectively dissolving hemicellulose and forming target products from its derivatives. Hemicellulose adheres to cellulose through hydrogen bonds and Van der Waals interactions, forming resistant networks; whereas covalent feruloyl ester-ether bridges link hemicellulose to lignin, complicating extraction. Therefore, developing methods for selective hemicellulose conversion is crucial to achieve high yield and selectivity without significantly decomposing cellulose and lignin (Agger et al., 2014; Carvalho et al., 2008; Hernández-Hernández et al., 2016; Langan et al., 2014; Morais et al., 2016).

Cottonseed contains approximately 27% hulls, 8% linters, 4% waste, 45% meal, 16% crude oil, and 10% acid detergent fiber, as well as other carbohydrate and mineral nutrients (Fig. 1) (National Cottonseed Products Association, n.d.). The major component of cottonseed is hulls, which are a viable feedstock of the lignocellulosic biomass. Studies show that cottonseed hulls (CSH) predominantly comprise protein (6.2%), holo-cellulose (65.6%),  $\alpha$ -cellulose (24.1-38.8%), hemicellulose (11.6-24.5%), and lignin (16.9-18.5%) (Dukare et al., 2023; Li et al., 2001) (Fig. 1). The substantial hemicellulose content in CSH holds significant potential for the

production of various high-value chemicals, such as furfural, a crucial platform chemical. It can be produced from CSH through a process involving hydrolysis and dehydration of hemicellulose, which is rich in pentosans (C-5 sugars, e.g., xylose) (Luo et al., 2019).

The global furfural market was valued at USD 556.74 million in 2022 and is expected to reach USD 767 million by 2028, with a projected compound annual growth rate of 7.0% from 2023 to 2030 (Grand View Research, 2022; Markets and Markets, 2023). Furfural is a common product derived from hemicellulose in raw biomass and serves as a crucial platform chemical in lignocellulosic biorefineries, produced through a process that involves the hydrolysis and dehydration of pentose sugars, primarily xylose and arabinose (Fig. 2). It can be further converted into fuels and various useful chemicals and is widely used in oil refining, plastics, pharmaceutical, and agrochemical industries (Mariscal et al., 2016). Optimization of the best conditions for furfural production was conducted using response surface methodology (RSM), which systematically evaluates and optimizes process variables. RSM models the relationships between multiple variables and the

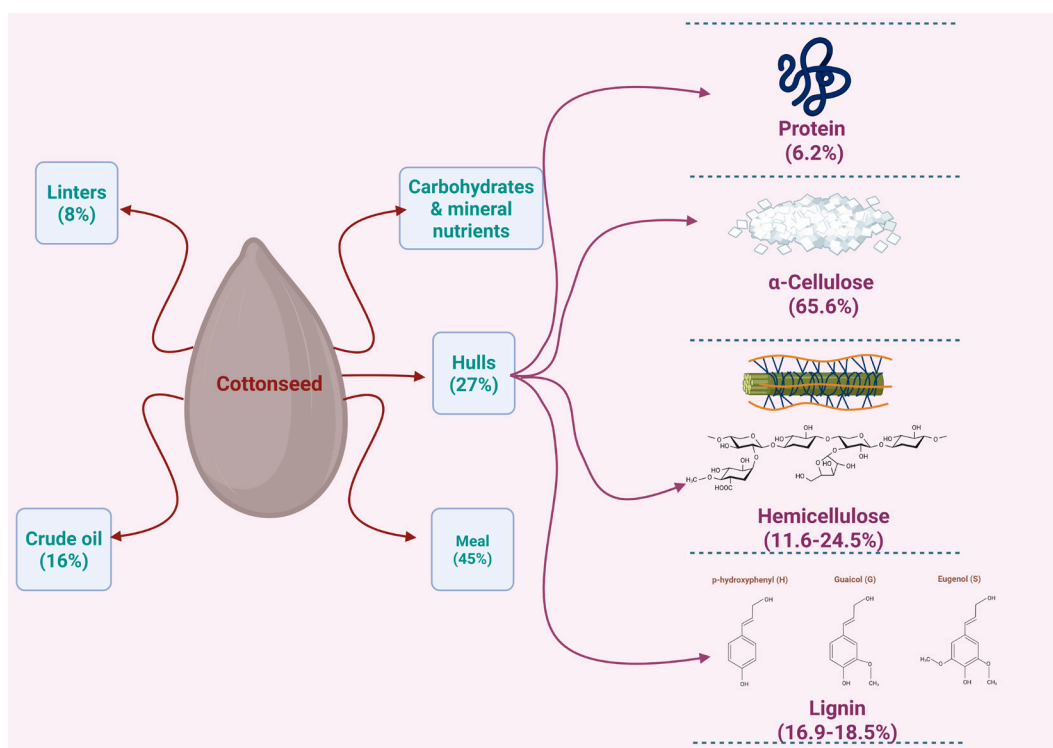


**Figure 1.** Components of cottonseed, which include linters (8%), crude oil (16%), meal (45%), and hulls (27%). Hulls, a major lignocellulosic biomass in cottonseed, comprise protein (6.2%),  $\alpha$ -cellulose (65.6%), hemicellulose (11.6-24.5%), and lignin (16.9-18.5%) (numerical values are taken from Dukare et al., 2023; Li et al., 2001).

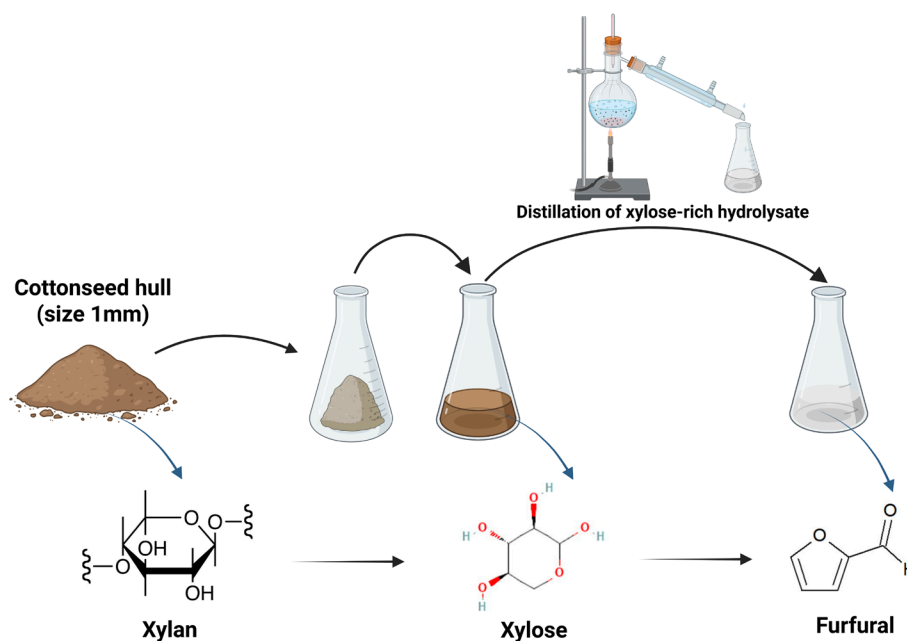


Figure 2. Conversion of cottonseed hulls to furfural.

response, identifying optimal conditions for desired outcomes. This approach is particularly useful for processes influenced by multiple variables and their interactions (Kumar et al., 2019). Achieving high yield of furfural from hemicellulose requires careful selection of solvent and catalyst. In this study, CSH was used, and the optimization was performed using RSM with a Box-Behnken design (BBD).

## MATERIALS AND METHODS

**Raw Materials and Chemicals.** CSH biomass was procured from Ginning Training Centre, Central Institute for Research on Cotton Technology (ICAR), Nagpur, India. The biomass was dried in an oven at 60 °C for 48 h, mechanically milled to 1 mm with the help of hammer mill from Dynamic AgroMachine (Model 9FO20-200, Maharashtra, India) and stored in airtight containers at room temperature for further analysis. The chemicals employed in this work were of analytical grade. Furfural (purity grade  $\geq 99.0\%$ ) was purchased from Sisco Research Laboratory (Mumbai, India). Sulfuric acid (EMPARTA®, purity 98%) was purchased from Merck Life Sciences Private Limited (Mumbai, India). All other chemicals and solvents used in the study were purchased from Hi Media Laboratories (Mumbai, India). A primary furfural standard stock was prepared by dissolving 100  $\mu\text{L}$  of furfural in 100 mL of water. Six secondary standards were prepared by diluting an appropriate

volume of the stock solution with water. A two-step dilution was used for obtaining low concentration standards that were used in generating a calibration curve.

**Pretreatment of Raw CSH and Acid Hydrolysis of Pretreated CSH.** CSH (5g) was placed in a conical flask (250 mL) adding sulfuric acid (1% v/v) to vary the ratio of acid to biomass (5:1 to 15:1). The flasks with the mixture were autoclaved for 30 min at 121 °C and 1 bar pressure. After 30 min the flasks were removed from the autoclave and cooled to room temperature. Once the mixture was cooled, hydrolysate and biomass were separated through filtration using Wattman no. 1 filter paper. Xylose-rich hydrolysate was prepared from the pretreated biomass, which was further subjected to acid hydrolysis using varying concentrations of sulfuric acid (2.5-7.5% v/v) at a constant ratio of 10:1 (acid:CSH). This mixture was placed in a round-bottom flask attached with condenser and heated at 100 °C for 30 to 90 min on a heating mantle. An aliquot of hydrolysate collected after hydrolysis was used for xylose estimation using orcinol reagent via UV-Vis spectrophotometer at 667 nm.

**Conversion of Xylose-Rich Hydrolysate to Furfural.** For the dehydration step, hydrolysate collected after acid pretreatment of CSH was mixed with xylose-rich hydrolysate obtained after acid hydrolysis of pretreated CSH biomass in a round-bottom flask along with sodium chloride (20 g). This

mixture was heated for 1 to 2 h on a heating mantle at 110 to 120 °C with a distillation setup attached to the flask for condensation and collection of furfural after dehydration. Furfural was collected in a cool amber bottle as it is light sensitive. Once collected, the liquid was filtered through Wattman no. 1 filter paper. Experiments were repeated in triplicate and standard deviation of the data was calculated. Xylose and furfural produced were estimated via UV-Vis spectrophotometric method at 667 and 275 nm, respectively. Xylose conversion and furfural yield were calculated according to standard graph equation of xylose and furfural. The process of production of furfural employed in this study is shown in Fig. 3.

#### Fourier Transform Infrared Spectroscopy.

The functional groups contained in the furfural were identified using Fourier transform infrared (FTIR) spectroscopy. FTIR spectra was obtained from commercial furfural and furfural extracted from CSH using FTIR system (Shimadzu IR Prestige-21, Kyoto, Japan) equipped with IR detector. One hundred  $\mu\text{L}$  of sample, pure furfural, pure xylose, and liquid collected after dehydration of xylose-rich hydrolysate were used for FTIR. One hundred  $\mu\text{L}$  sample amounts resulted in maximum relative band intensity and no peak saturation. Data were then collected over the range 4,000 to 400  $\text{cm}^{-1}$  obtained by averaging 45

scans with a resolution of 4  $\text{cm}^{-1}$ . The analysis was performed using IRSolution software. The functional groups were then interpreted by comparing the peaks obtained to previous articles and a functional group chart.

**Optimization of Furfural Production Through RSM Using BBD.** The experimental design for the response surface was conducted using Design-Expert software. This involved three independent variables: pre-treatment (A) using a varying ratio (5:1 to 15:1) of 1%  $\text{H}_2\text{SO}_4$  to CSH (1%  $\text{H}_2\text{SO}_4$ :CSH); acid hydrolysis (B) using a varying concentration (2.5-7.5%) of  $\text{H}_2\text{SO}_4$  to CSH (%  $\text{H}_2\text{SO}_4$ :CSH); and reaction time (C) ranging from 30 to 90 min. The experimental design consisted of 12 factorial points (non-center points), as seen in Table 1. Five replicates at the midpoint (A = 0, B = 0, C = 0) were used to estimate experimental error and pure error (Table 2).

For acid hydrolysis, the ratio of acid ( $\text{H}_2\text{SO}_4$ ) to CSH was maintained at 10:1 for all tested samples. The coded and actual values of various input factors are presented in Table 1. The dependent response, furfural yield (%), was evaluated following the BBD approach of RSM. BBD resulted in 17 experiments with three independent variables as shown in Table 2. The response surface plots generated from BBD revealed significant interactions among pretreatment

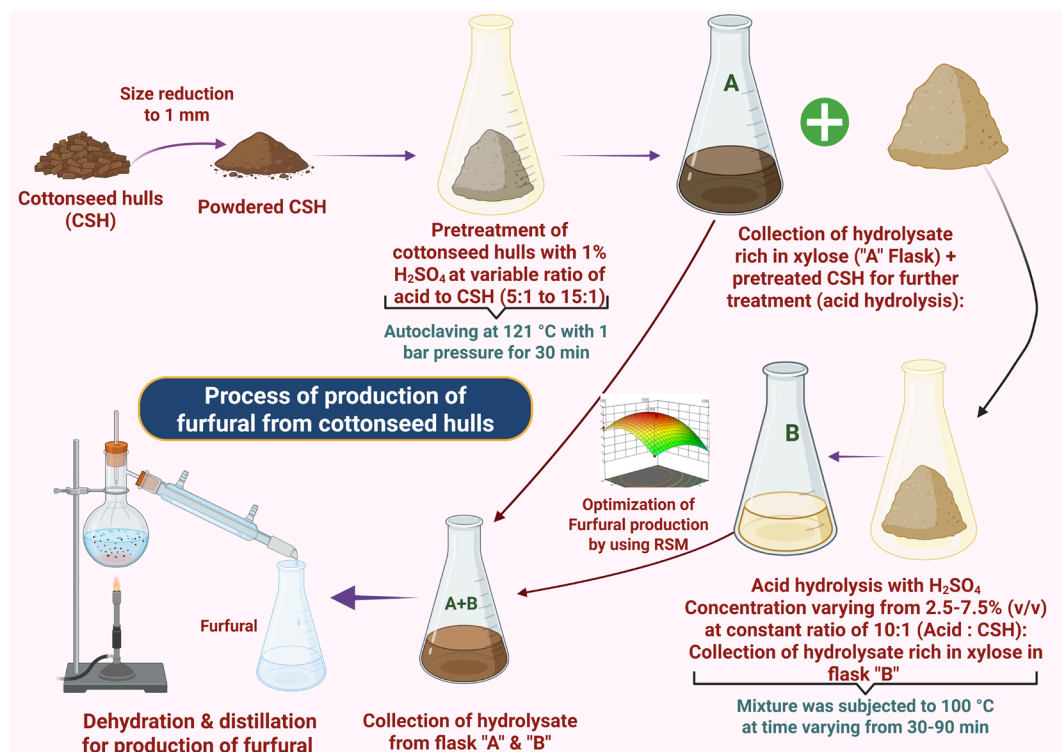


Figure 3. Process protocol for production of furfural from cottonseed hulls.

Table 1. Experimental factor levels

Independent variable	Units	Symbol	Coded and Actual Level		
			-1	0	+1
Pretreatment condition (1% $\text{H}_2\text{SO}_4$ :CSH)	mL/g	A	5	10	15
Acid hydrolysis condition (% $\text{H}_2\text{SO}_4$ :CSH)	mL/g	B	2.50	5.00	7.50
Reaction time	min	C	30	60	90

Table 2. Three-level, three-factor experimental design. Experimental conditions and response (furfural yield) results

Std	Run	A-Pretreatment (1% $\text{H}_2\text{SO}_4$ :CSH)	B-Acid Hydrolysis (% $\text{H}_2\text{SO}_4$ :CSH)	C-Reaction Time	Response: Furfural Yield
		(mL/g)	(mL/g)	(min)	(%)
17	1	0 (10)	0 (5)	0 (60)	13.74
7	2	-1 (5)	0 (5)	+1 (90)	8.43
6	3	+1 (15)	0 (5)	-1 (30)	4.36
16	4	0 (10)	0 (5)	0 (60)	14.01
14	5	0 (10)	0 (5)	0 (60)	13.20
3	6	-1 (5)	+1 (7.5)	0 (60)	10.89
1	7	-1 (5)	-1 (2.5)	0 (60)	7.31
13	8	0 (10)	0 (5)	0 (60)	14.21
15	9	0 (10)	0 (5)	0 (60)	12.88
10	10	0 (10)	+1 (7.5)	-1 (30)	7.64
12	11	0 (10)	+1 (7.5)	+1 (90)	12.28
4	12	+1 (15)	+1 (7.5)	0 (60)	11.41
8	13	+1 (15)	0 (5)	+1 (90)	12.82
5	14	-1 (5)	0 (5)	-1 (30)	7.91
11	15	0 (10)	-1 (2.5)	+1 (90)	8.73
9	16	0 (10)	-1 (2.5)	-1 (30)	2.35
2	17	+1 (15)	-1 (2.5)	0 (60)	4.25

(1%  $\text{H}_2\text{SO}_4$ :CSH), acid hydrolysis (%  $\text{H}_2\text{SO}_4$ :CSH), and reaction time (Table 3).

A series of 17 experiments were conducted following a three-level, three-factor experimental design to optimize furfural yield, considering pretreatment (Factor A), acid hydrolysis (Factor B), and reaction time (Factor C) as independent variables. We chose sulfuric acid ( $\text{H}_2\text{SO}_4$ ) for pretreatment and acid hydrolysis of CSH for furfural production based on the findings reported by Lee and Wu (2021). Their review highlighted that sulfuric acid, used in the Dupont process with corn cobs, yielded the highest production of furfural among various industrial processes (Sherif et al., 2021). Other reputed industries such as Westpro, Supra Yield®, and Quaker Oats also used  $\text{H}_2\text{SO}_4$  and achieved furfural yields ranging from 35 to 70%. This suggests that  $\text{H}_2\text{SO}_4$  is an effective catalyst, which likely enhances the efficiency and yield of furfural production.

**Statistical Analysis.** The data on the percentage yield of furfural from CSH under different conditions were subjected to ANOVA, considering the varying conditions of pretreatment, acid hydrolysis, and time, using Design-Expert software, (Minnesota, USA). Significant differences among the various treatments were identified according to the ANOVA results and are presented in Table 3. The statistical significance of all other variables was calculated based on the standard deviation of triplicate tests performed for each specific analysis.

## RESULTS AND DISCUSSION

**Optimization of Furfural Production Through RSM Using BBD.** The results from the current study demonstrated significant variability in furfural yields based on different experimental conditions. Under intermediate coded conditions (0,0,0), furfural yields



**Table 3. Model summary statistics: ANOVA (for significance values), regression coefficient, coefficient of determination ( $R^2$ ), and F-test value of the second order polynomial models for the furfural yield**

Source	Furfural (Regression coefficients)	Sum of Squares	df	Mean Square	F-value	<i>p</i> -value <sup>x</sup>
Intercept	13.6064					
Model		222.46	9	24.72	47.54 y	<0.0001***
A-Pretreatment <sup>z</sup>	-0.213056	0.3631	1	0.3631	0.6984	0.4309
B-Acid Hydrolysis <sup>z</sup>	2.44944	48.00	1	48.00	92.31	<0.0001***
C-Reaction time	2.5	50.00	1	50.00	96.16	<0.0001***
AB	0.893056	3.19	1	3.19	6.14	0.0424**
AC	1.98306	15.73	1	15.73	30.25	0.0009***
BC	-0.434722	0.7559	1	0.7559	1.45	0.2671
A <sup>2</sup>	0.0004	21.42	1	21.42	41.20	0.0004***
B <sup>2</sup>	< 0.0001	35.03	1	35.03	67.38	<0.0001***
C <sup>2</sup>	< 0.0001	37.17	1	37.17	71.49	<0.0001***
Residual		3.64	7	0.5199		
Lack of Fit <sup>w</sup>		2.40	3	0.7984	2.57	0.1924
Pure Error		1.24	4	0.3111		
Cor Total		226.10	16			
R <sup>2</sup>	0.984					
Adj R <sup>2</sup>	0.963					
Pred R <sup>2v</sup>	0.822					
Adeq Precision <sup>u</sup>	20.32					
Std. Dev.	0.7211					
C.V. %	7.37					

<sup>z</sup>A-Pretreatment (1% H<sub>2</sub>SO<sub>4</sub>:CSH), B-Acid Hydrolysis (% H<sub>2</sub>SO<sub>4</sub>:CSH)<sup>y</sup>The Model F-value of 47.54 implies the model is significant. There is only a 0.01% chance that an F-value this large could occur due to noise.<sup>x</sup>*P*-values < 0.0500 indicate model terms are significant. *P*-values > 0.1000 indicate the model terms are not significant.<sup>w</sup>The lack-of-fit F-value of 2.57 implies the lack of fit is not significant relative to the pure error. There is a 19.24% chance that a lack-of-fit F-value this large could occur due to noise. Non-significant lack of fit is good.<sup>v</sup>The Predicted R<sup>2</sup> of 0.8219 is in reasonable agreement with the Adjusted R<sup>2</sup> of 0.9632; i.e., the difference is less than 0.2.<sup>u</sup>Adeq Precision measures the signal-to-noise ratio. A ratio greater than 4 is desirable. Ratio of 20.324 indicates an adequate signal.

were consistently observed at approximately 13.74, 14.01, and 13.20% for Runs 1, 4, and 5, respectively. The initial step involved pre-treating the biomass to produce a hydrolysate rich in xylose, which was then dehydrated in the subsequent step. Decreasing pretreatment (Factor A) resulted in lower yields, as seen in Run 2 with a yield of 8.43%, and was even more pronounced when combined with decreased acid hydrolysis (Factor B) in Run 7, yielding only 7.31%. Conversely, increasing pretreatment ratio (1% H<sub>2</sub>SO<sub>4</sub>:CSH) to 15:1 also led to significant yield reductions, notably in Runs 3 and 17, which yielded 4.36 and 4.25%, respectively. This reaction might

be due to interaction of Factor A with Factors B and C. An optimized concentration of sulfuric acid can lead to depolymerizing the hemicellulose, increasing the availability of fermentable sugars. This process not only facilitates the release of xylose but also promotes the subsequent dehydration of xylose to furfural, thereby improving the overall efficiency and yield of furfural production. Seventeen experiments conducted as part of BBD showed that using 1% H<sub>2</sub>SO<sub>4</sub> at a 10:1 ratio (acid:CSH) was the most effective for increasing the yield of furfural. Raman and Gnansounou (2015) reported similar results where they used 1.025% sulfuric acid to achieve

release of xylose and subsequent higher production of furfural after dehydration.

When analyzing the effect of acid hydrolysis, increasing acid concentration while maintaining pretreatment (0) and reaction time (0) yielded mixed results. For example, Run 6 with increased acid hydrolysis (+1), (7.5% [v/v] of H<sub>2</sub>SO<sub>4</sub> at 10:1 acid:CSH) showed a modest yield of 10.89%, whereas combining increased acid hydrolysis with increased reaction time (+1) in Run 11 resulted in a higher yield of 12.28%. However, extreme combinations, such as intermediate pretreatment (0) and acid hydrolysis (-1) and time (-1) in Run 16, led to a drastically reduced yield of 2.35%. The acid concentration for the second stage (acid hydrolysis) of releasing xylose in the hydrolysate was kept on the lower side, varying from 2.5 to 7.5%, to avoid the possible degradation of the pentose sugars.

The reaction time (Factor C) also influenced yields. For example, the highest pretreatment condition (+1) and acid hydrolysis (+1) with intermediate reaction time (0) in Run 12 yielded 11.41%. On the other hand, decreasing reaction time (-1) while maintaining intermediate pretreatment (0) and increased acid hydrolysis (+1 [7.5% (v/v) H<sub>2</sub>SO<sub>4</sub>]) resulted in a lower yield of 7.64% in Run 10. Overall, the results indicate that moderate/intermediate conditions (0, 0, 0) for pretreatment, acid hydrolysis, and reaction time respectively, tend to favor higher furfural yields. Extreme variations in any of these factors, particularly when combined, tend to reduce the yield significantly. The highest yields were observed under conditions close to the central points of the experimental design, suggesting that balancing these factors is crucial for optimizing furfural production. Further statistical analysis of the results was crucial to establish the validity and significance of the results. ANOVA and RSM were used to elucidate the interactions between these factors and refine the optimal conditions for maximum furfural yield.

**ANOVA, P-Values, and Other Statistical Parameters for Visualization of the Quadratic Model.** To visualize the quadratic model, ANOVA, *p*-values, and coefficient of determination (*R*<sup>2</sup>) were employed using Design-Expert 13.0. The 3D surface plots for the response (furfural yield) were also generated to aid in this analysis. The ANOVA results for the quadratic model applied to the furfural yield from CSH are presented in Table 3. The model demonstrates significant statistical relevance, with a model *F*-value of 47.54, indicating that there is

only a 0.01% chance that such a large *F*-value could occur due to noise. The coefficient of determination (*R*<sup>2</sup>) was found to be 0.9839, suggesting a strong correlation between the model and the experimental data. This high *R*<sup>2</sup> value implies that 98.39% of the variability in furfural yield can be explained by the model, confirming its robustness. The adjusted *R*<sup>2</sup> of 0.9632, which is in close agreement with the predicted *R*<sup>2</sup> of 0.8219, further validates the model's predictive capability, showing that the model is not overfitted and can reliably predict new data points within the experimental range.

The data in Table 2 were analyzed by regression to obtain one regression model for furfural yield with different factor coding values, as shown by the equation:

$$\text{Furfural yield} = 13.6064 - 0.21 * A + 2.45 * B + 2.5 * C + 0.89 * AB + 1.98 * AC - 0.43 * BC - 2.25558 * A^2 + -2.88 * B^2 - 2.97 * C^2$$

The model was subjected to regression and analysis of variance and the results are shown in Table 3.

**Significant Model Terms.** The analysis identified several significant model terms, each contributing to the understanding of how different factors influence furfural yield. These significant terms are characterized by *p*-values < 0.0500, highlighting their strong effect on the response variable. Acid hydrolysis (% H<sub>2</sub>SO<sub>4</sub>:CSH) (B) exhibited an *F*-value of 92.31 and a *p*-value < 0.0001, indicating a highly significant impact on furfural yield. This suggests that variations in the concentration of acid hydrolysis are crucial for the production of furfural. The large *F*-value enhances the necessity of optimizing this factor to enhance yield. The results of 17 RSM experiments indicate that an increase in the concentration of acid leads to a higher final yield of furfural. However, harsher conditions or high concentration of acid could lead to degradation of furfural. Harsh acidic conditions, such as those with high concentrations of sulfuric acid, increase the rate of xylose dehydration to furfural but also accelerate furfural decomposition. This leads to reduced furfural yields and the formation of unwanted by-products. Therefore, to maximize furfural production and minimize its degradation, sulfuric acid concentration for standardization was not more than 7.5%. A study by Kim et al. (2012) demonstrated that the use of maleic acid as the catalyst minimized furfural degradation reactions due to the less harsh nature of the catalyst compared to the mineral acids. Reaction time (C) is another critical factor with an *F*-

value of 96.16 and  $p$ -value  $< 0.0001$ . The significant effect of reaction time implies that the duration of the reaction plays a pivotal role in determining the furfural yield. This necessitates precise control and optimization of reaction time to maximize production efficiency. Reaction time of 60 min was found optimal for furfural production (34 wt%) from pine wood (Steinbach et al., 2017); similarly in the current study for CSH, maximum yield was attained at reaction time of 60 and 90 min, indicating the type of lignocellulosic biomass is a deciding factor. This highlights the importance of optimizing reaction time based on biomass type.

Interaction between acid hydrolysis and pretreatment (AB) had an F-value of 6.14 and a  $p$ -value of 0.0424, indicating a significant combined effect of acid hydrolysis and pretreatment on yield. This interaction highlights the importance of considering the synergistic effects of these two factors, rather than evaluating them in isolation. Understanding this interaction can lead to more nuanced and effective optimization strategies. Interaction between acid hydrolysis and reaction time (AC) showed an F-value of 30.25 and a  $p$ -value of 0.0009, pointing to a strong interaction effect. This significant interaction suggests that the optimal reaction time is dependent on the level of acid hydrolysis applied. Thus, the interaction between these two factors must be carefully balanced to achieve the highest possible yield. Padilla-Rascón et al. (2020) suggested that interaction of independent factors has great significance in improving the yield of the furfural from xylose. The quadratic terms for acid hydrolysis ( $B^2$ ), pretreatment ( $A^2$ ), and reaction time ( $C^2$ ) were all highly significant, with F-values of 41.20, 67.38, and 71.49, respectively, and  $p$ -values of  $< 0.0001$ .

**Non-Significant Model Terms.** Several terms were identified as non-significant, indicated by  $p$ -values greater than 0.1000, suggesting that within the experimental range, these factors did not have a substantial impact on the response variable. The pretreatment condition (A) had an F-value of 0.6984 and a  $p$ -value of 0.4309, indicating that variations in pretreatment within the studied range do not significantly affect furfural yield. This suggests that although pretreatment is necessary, its specific level within the tested range is less critical compared to other factors. Interaction between acid hydrolysis (B) and reaction time (C) terms showed an F-value of 1.45 and a  $p$ -value of 0.2671, indicating that the combined effect of B and C is not significant within

the experimental range. This finding implies that these two factors influence the yield independently rather than synergistically within the tested levels.

**Model Adequacy.** The lack-of-fit test, which evaluates the model's adequacy, was found to be non-significant with an F-value of 2.57 and  $p$ -value of 0.1924. This indicates that the model fits the experimental data well and that there is no significant error in the model predictions. Therefore, the model's predictions are reliable within the range of the experimental variables tested. Additionally, the adequate precision value of 20.324, which measures the signal-to-noise ratio, indicates an adequate signal. A ratio greater than 4 is desirable, and the obtained value suggests that this model can be used effectively to navigate the design space.

In summary, the ANOVA results enhance the significance of the quadratic model in predicting furfural yield from CSH. The high F-values and low  $p$ -values for factors B (acid hydrolysis), C (reaction time), their interactions (AB and AC), and their quadratic terms ( $A^2$ ,  $B^2$ , and  $C^2$ ) indicate that these factors have a substantial impact on furfural yield. This suggests that optimizing acid hydrolysis concentration and reaction time, both individually and in combination, is crucial for maximizing furfural production. Conversely, the pretreatment factor (A) and its interaction with acid hydrolysis (BC) did not significantly influence the yield within the tested range, implying that these factors are less critical within the specified conditions. This detailed statistical analysis supports the robustness of the quadratic model and highlights the critical parameters for optimizing furfural production from CSH.

**Response Surface and Contour Plots to Visualize the Interaction Between Input Factors and Their Relation to Furfural Yield.** To study the interaction between input factors and their relationship to furfural yield, response surface, and contour plots were generated using Design-Expert software. The input factors included were pretreatment concentration, acid hydrolysis concentration, and reaction time. The criteria and goals for these factors, along with their respective ranges and importance levels, are summarized in Table 4.

**Interaction Between A (Pretreatment) and B (Acid Hydrolysis).** In the response surface plot (Fig. 4a), the interaction between pretreatment (A) and acid hydrolysis (B) on furfural yield is illustrated. The surface indicates that furfural yield increases with both A and B up to a certain point, after which



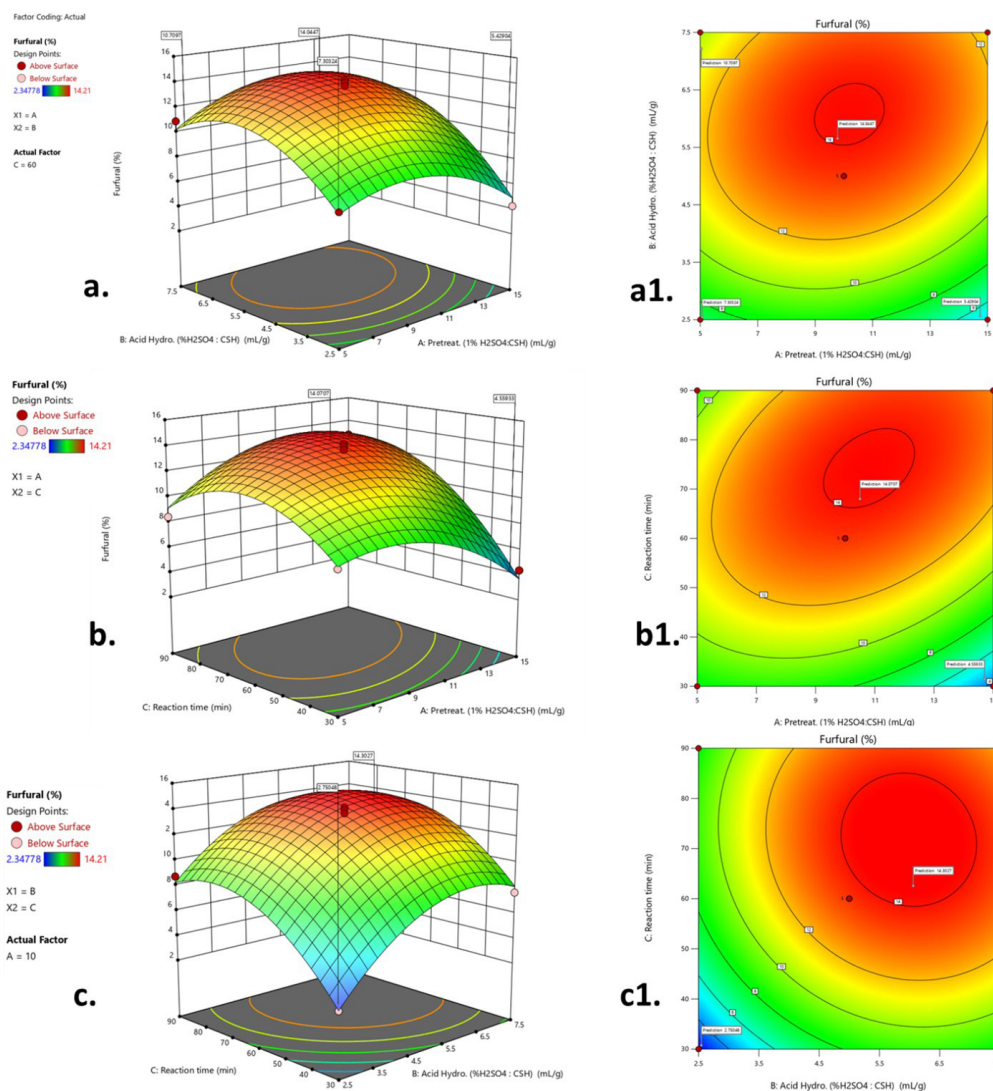


**Figure 4.** Response surface curves and contour plots of furfural yield (%) from cottonseed hulls for studying the interaction of input factors.

it stabilizes. The contour plot (Fig. 4a1) reinforces this, showing concentric rings where the highest yields (red area) are achieved with a pretreatment approximately 11 to 12 mL/g and acid hydrolysis approximately 5.5 to 6.5 mL/g. The interaction is significant, as both factors need to be optimized simultaneously to achieve maximum yield.

**Interaction Between A (Pretreatment) and C (Reaction Time).** In the response surface plot (Fig. 4b), the interaction between pretreatment (A) and reaction time (C) on furfural yield is presented. The surface suggests that increasing the reaction time initially boosts furfural yield, but this effect plateaus beyond 70 to 90 min. Similarly, pretreatment approximately 10 to 13 mL/g maximizes yield. The contour plot (Fig. 4b1) shows a red region indicat-

ing optimal conditions, suggesting that both factors interact positively up to an optimal point, beyond which the yield remains constant.

**Interaction Between B (Acid Hydrolysis) and C (Reaction Time).** The response surface plot (Fig. 4c) displays the interaction between acid hydrolysis (B) and reaction time (C) on furfural yield. The plot shows an increase in yield with increasing reaction time and acid hydrolysis concentration until an optimal point. Beyond this, the yield stabilizes. The contour plot (Fig. 4c1) indicates that the highest furfural yield (red region) is achieved with acid hydrolysis at 5 to 7 mL/g and reaction time approximately 60 to 85 min, demonstrating a synergistic interaction between these factors.

The response surface and contour plots (Fig. 4) illustrate the importance of optimizing pretreatment, acid hydrolysis, and reaction time simultaneously to maximize furfural yield. The interaction plots reveal that all three factors have significant combined effects, with specific optimal ranges that ensure the highest production of furfural.

**Optimization and Validation of Processing Input Factors and Predicted Furfural Yield.** The optimum processing conditions for the production of furfural were determined using Design-Expert software. The main criterion for optimization was to achieve the highest yield of furfural. The optimized parameters identified were: pretreatment (1%  $\text{H}_2\text{SO}_4$ ) at 11.73 mL/g, acid hydrolysis (%  $\text{H}_2\text{SO}_4$ ) at 6.74%, and a reaction time of 81.2 min. The predicted furfural yield from RSM was validated with a desirability score of 1, indicating perfect optimization (Fig. 5). To validate the optimized conditions, a confirmation run was performed, yielding a furfural production of 12.8%, which aligns with the model-predicted value of 14.34%. This result confirms the reliability and predictive accuracy of the developed model. The results validated the RSM model, demonstrating its effectiveness in predicting the optimum conditions for maximizing furfural production.

**FTIR Analysis of Optimized Sample of Furfural.** The FTIR spectroscopy analysis was conducted to compare the functional groups present in a standard furfural sample (black spectrum) with those in furfural produced from CSH (red spectrum) (Fig. 6). The spectra reveal several key similarities and dif-

ferences that provide insights into the composition of the produced furfural. The broad O-H stretching peak observed at approximately  $3,320\text{ cm}^{-1}$  in both the standard and produced furfural indicates the presence of hydroxyl groups or moisture. However, the produced furfural shows a slightly less intense peak in this region, suggesting a lower moisture content or fewer hydroxyl groups. Both spectra exhibit C-H stretching vibrations between  $3,000$  to  $2,800\text{ cm}^{-1}$ , characteristic of aldehyde and aromatic C-H bonds, with similar intensity and positioning, indicating comparable levels of these bonds in both samples.

A sharp peak at approximately  $1,700\text{ cm}^{-1}$ , indicative of the carbonyl group ( $\text{C}=\text{O}$ ) in the aldehyde functional group of furfural is present in both spectra. The produced furfural, however, displays a slightly broader and shifted peak that could be due to interactions with other functional groups or impurities. Additionally, peaks corresponding to aromatic  $\text{C}=\text{C}$  stretching between  $1,600$  to  $1,500\text{ cm}^{-1}$  are evident in both samples, though the produced furfural shows slightly less intense peaks, suggesting a possible variation in aromatic content. The fingerprint region ( $1,500$ - $500\text{ cm}^{-1}$ ) of both spectra exhibits a complex pattern of peaks corresponding to various bending and stretching vibrations of C-H, C-O, and C-C bonds. A similar band pattern was observed by Sashikala and Ong (2007) from furfural produced from rice straw. Although the overall patterns are similar, the produced furfural shows less intense and somewhat broadened peaks, indicating potential impurities or structural differences. These variations

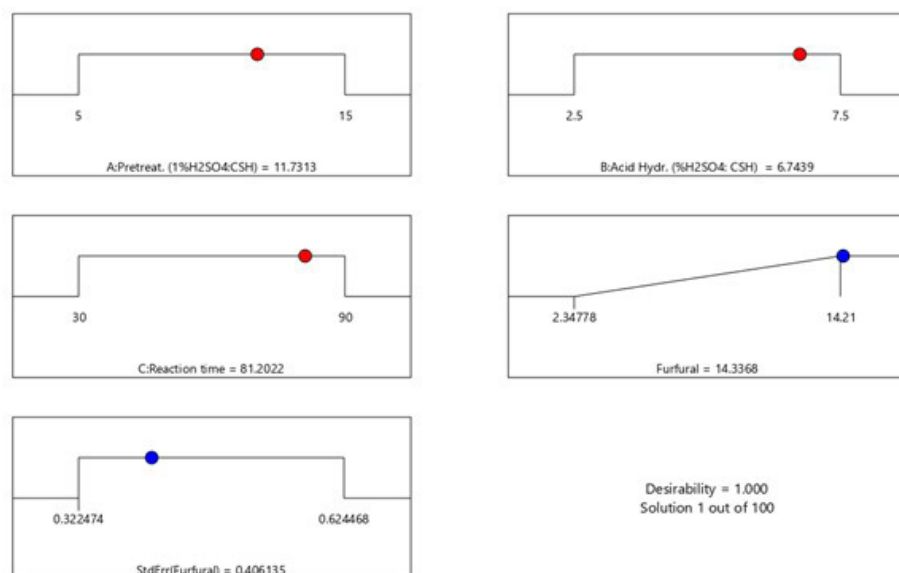
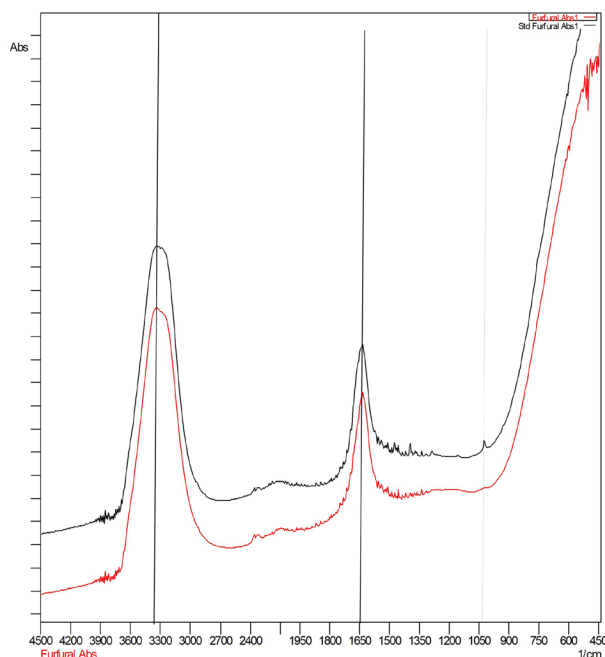


Figure 5. Optimization of input conditions for furfural production from cottonseed hulls by Design-Expert.



**Figure 6.** FTIR absorption spectra of standard furfural (black) and furfural produced from cottonseed hulls (red).

could be attributed to incomplete purification or the presence of other organic compounds from the CSH. Considering the findings it is evident that the furfural produced from CSH contains the major characteristic functional groups of furfural as evidenced by the similarity in the primary absorption peaks with standard furfural. However, the observed differences in peak intensity, sharpness, and slight shifts suggest the presence of impurities or structural variations in the produced sample.

## CONCLUSIONS

This study successfully demonstrates the effective use of BBD and RSM to optimize furfural production from CSH, an abundant lignocellulosic biomass. By systematically investigating the effects of pretreatment conditions, acid hydrolysis concentration, and reaction time, we identified optimal conditions that maximize furfural yield. The optimized parameters: pretreatment condition of 11.73:1 (1%  $\text{H}_2\text{SO}_4$ :CSH), acid hydrolysis condition of 6.74% (%  $\text{H}_2\text{SO}_4$ :CSH), and a reaction time of 81.2 min, resulted in maximum furfural yield of 14.34%. Statistical analysis via ANOVA confirmed the significance of the model, enhancing the reliability of our optimization approach. The results also demonstrated the potential of CSH as a sustainable and economically viable source for furfural production, contributing

to the broader objective of biomass conversion technologies. This study not only demonstrates an efficient method for maximizing furfural yield but also highlights the value of agricultural by-products in the biorefinery industry. By advancing the optimization of production processes, this research supports the sustainable production of high-value chemicals from renewable resources, aligning with global efforts to develop green and sustainable industrial practices.

Future research should focus on scaling up the optimized process to pilot and industrial scales to assess practical and economic feasibility. Exploring the applicability of this method to other lignocellulosic biomasses can expand feedstock versatility. Integrating furfural production with other biorefinery processes could enhance overall economic efficiency. Investigating alternative catalysts could improve selectivity and yield, reducing environmental impact and costs. Comprehensive life cycle assessments will ensure environmental sustainability. Additionally, exploring the use of by-products can contribute to a zero-waste biorefinery model. Addressing these areas will strengthen the efficiency and sustainability of furfural production from CSH, promoting the broader adoption of renewable resources in the biorefinery industry.

## ACKNOWLEDGMENTS

The authors are thankful to Director, ICAR-Central Institute for Research on Cotton Technology, Mumbai, India for providing all facilities and funding to carry out this research. I also acknowledge that figures 1, 2, and 3 were created in BioRender (Toronto, Canada).

## REFERENCES

- Agger, J.W., T. Isaksen, A. Várnai, S. Vidal-Melgosa, W.G.T. Willats, R. Ludwig, S.J. Horn, V.G.H. Eijsink, and B. Westereng. 2014. Discovery of LPMO activity on hemicelluloses shows the importance of oxidative processes in plant cell wall degradation. *Proc. Natl. Acad. Sci.* 111(17):6287–6292. <https://doi.org/10.1073/pnas.1323629111>
- Ajao, O., M. Marinova, O. Savadogo, and J. Paris. 2018. Hemicellulose based integrated forest biorefineries: Implementation strategies. *Indus. Crops Prod.* 126:250–260. <https://doi.org/10.1016/j.indcrop.2018.10.025>

- Carvalho, F., L.C. Duarte, and F. Gírio. 2008. Hemicellulose biorefineries: a review on biomass pretreatments. *J. Sci. Indust. Res.* 67:849–864.
- Desrochers, P., and J. Szurmak. 2017. Long distance trade, locational dynamics and by-product development: Insights from the history of the American cottonseed industry. *Sustainability*. 9(4):579. <https://doi.org/10.3390/su9040579>
- Dukare, A., K. Sharma, V. Nadanathangam, L. Nehete, and S. Saxena. 2023. Valorization of cotton seed hulls as a potential feedstock for the production of thermostable and alkali-tolerant bacterial xylanase. *BioEnergy Res.* 17(1):173–186. <https://doi.org/10.1007/s12155-023-10646-y>
- Grand View Research. 2022. Furfural market size, share & trends analysis report by application (furfuryl alcohol, solvents, pharmaceuticals, chemical intermediates), by raw material (corn cob, rice husk, bagasse), by region, and segment forecasts. 2023 - 2030 [Online]. Available at <https://www.grandviewresearch.com/industry-analysis/furfural-market> (verified 10 April 2025).
- Hernández-Hernández, H.M., J.J. Chanona-Pérez, A. Vega, P. Ligerio, J.A. Mendoza-Pérez, G. Calderón-Domínguez, E. Terrés, and R.R. Farrera-Rebollo. 2016. Acetosolv treatment of fibers from waste agave leaves: Influence of process variables and microstructural study. *Indus. Crops Prod.* 86:163–172. <https://doi.org/10.1016/j.indcrop.2016.03.043>
- Kim, E.S., S. Liu, M.M. Abu-Omar, and N.S. Mosier. 2012. Selective conversion of biomass hemicellulose to furfural using maleic acid with microwave heating. *Ener. Fuels*. 26(2):1298–1304. <https://doi.org/10.1021/ef2014106>
- Kumar, M., A. Dahuja, A. Sachdev, C. Kaur, E. Varghese, S. Saha, and K.V.S.S. Sairam. 2019. Evaluation of enzyme and microwave-assisted conditions on extraction of anthocyanins and total phenolics from black soybean (*Glycine max* L.) seed coat. *Inter. J. Biol. Macromolecules*. 135:1070–1081. <https://doi.org/10.1016/j.ijbiomac.2019.06.034>
- Langan, P., L. Petridis, H.M. O'Neill, S.V. Pingali, M. Foston, Y. Nishiyama, R. Schulz, B. Lindner, B.L. Hanson, S. Harton, W.T. Heller, V. Urban, B.R. Evans, S. Gnana-karan, A.J. Ragauskas, J.C. Smith, and B.H. Davison. 2014. Common processes drive the thermochemical pretreatment of lignocellulosic biomass. *Green Chem.* 16(1):63–68. <https://doi.org/10.1039/C3GC41962B>
- Lee, C.B.T.L., and T.Y. Wu. 2021. A review on solvent systems for furfural production from lignocellulosic biomass. *Renew. Sustain. Ener. Rev.* 137:110172. <https://doi.org/10.1016/j.rser.2020.110172>
- Li, X., Y. Pang, and R. Zhang. 2001. Compositional changes of cottonseed hull substrate during *P. ostreatus* growth and the effects on the feeding value of the spent substrate. *Bioresource Tech.* 80(2):157–161. [https://doi.org/10.1016/S0960-8524\(00\)00170-X](https://doi.org/10.1016/S0960-8524(00)00170-X)
- Lu, L., W. Fan, X. Meng, L. Xue, S. Ge, C. Wang, S.Y. Foong, C.S.Y. Tan, C. Sonnee, M. Aghbashlo, M. Tabatabaei, and S.S. Lam. 2023. Current recycling strategies and high-value utilization of waste cotton. *Sci. Total Envir.* 856(1):158798. <https://doi.org/10.1016/j.scitotenv.2022.158798>
- Luo, Y., Z. Li, X. Li, X. Liu, J. Fan, J.H. Clark, and C. Hu. 2019. The production of furfural directly from hemicellulose in lignocellulosic biomass: A review. *Catalysis Today*. 319:14–24. <https://doi.org/10.1016/j.cattod.2018.06.042>
- Mariscal, R., P. Maireles-Torres, M. Ojeda, I. Sádaba, and M.L. Granados. 2016. Furfural: a renewable and versatile platform molecule for the synthesis of chemicals and fuels. *Energy Environ. Sci.* 9(4):1144–1189. <https://doi.org/10.1039/C5EE02666K>
- Markets and Markets. 2023. Furfural market by raw material (sugarcane bagasse, corncob, rice husk), application (derivatives, solvents), end-use industry (agriculture, paint & coatings, pharmaceuticals, food & beverages, refineries), and region - Global forecast to 2028. Report Code: CH 7382. Available at <https://www.marketsandmarkets.com/Market-Reports/furfural-market-101056456.html> (verified 29 May 2025).
- Morais, A.R.C., M.D.D.J. Matuchaki, J. Andreus, and R. Bogel-Lukasik. 2016. A green and efficient approach to selective conversion of xylose and biomass hemicellulose into furfural in aqueous media using high-pressure CO<sub>2</sub> as a sustainable catalyst. *Green Chem.* 18(10):2985–2994. <https://doi.org/10.1039/C6GC00043F>
- National Cottonseed Products Association. n.d. Products [Online]. Available at <https://www.cottonseed.com/products/> (verified 10 April 2025).
- Padilla-Rascón, C., J.M. Romero-García, E. Ruiz, and E. Castro. 2020. Optimization with response surface methodology of microwave-assisted conversion of xylose to furfural. *Molecules*. 25(16):3574. <https://doi.org/10.3390/molecules25163574>
- Raman, J.K., and E. Gnansounou. 2015. Furfural production from empty fruit bunch - A biorefinery approach. *Indust. Crops Prod.* 69:371–377. <https://doi.org/10.1016/j.indcrop.2015.02.063>



- Scapini, T., M.S.N. dos Santos, C. Bonatto, J.H.C. Wancura, J. Mulinari, A.F. Camargo, N. Klanovicz, G.L. Zabot, M.V. Tres, G. Fongaro, and H. Treichel. 2021. Hydrothermal pretreatment of lignocellulosic biomass for hemicellulose recovery. *Bioresource Tech.* 342:126033. <https://doi.org/10.1016/j.biortech.2021.126033>
- Sashikala, M., and H.K. Ong. 2007. Synthesis and identification of furfural from rice straw. *J. Trop. Agric. Food Sci.* 35(1):165.
- Sherif, N., M. Gadalla, and D. Kamel. 2021. Acid-hydrolysed furfural production from rice straw bio-waste: Process synthesis, simulation, and optimisation. *South African J. Chem. Engin.* 38(1):34–40. <https://doi.org/10.1016/j.sajce.2021.08.002>
- Steinbach, D., A. Kruse, and J. Sauer. 2017. Pretreatment technologies of lignocellulosic biomass in water in view of furfural and 5-hydroxymethylfurfural production - a review. *Biomass Conversion Biorefinery.* 7:247–274. <https://doi.org/10.1007/s13399-017-0243-0>
- United States Department of Agriculture, Economic Research Service [USDA ERS]. 2014. Oil Crops Yearbook [Online database]. Available at <https://www.ers.usda.gov/data-products/oil-crops-yearbook/> (verified 11 April 2025).
- Voora, V., S. Bermudez, J.J. Farrell, C. Larrea, and E. Luna. 2023. Cotton prices and sustainability [Online]. Sustainable Commodities Marketplace Series. International Institute for Sustainable Development. Available at <https://www.iisd.org/system/files/2023-01/2023-global-market-report-cotton.pdf> (verified 11 April 2025).
- Wierzbicki, M.P., V. Maloney, E. Mizrachi, and A.A. Myburg. 2019. Xylan in the middle: understanding xylan biosynthesis and its metabolic dependencies toward improving wood fiber for industrial processing. *Front. Plant Sci.* 10:423929. <https://doi.org/10.3389/fpls.2019.00176>